

Processing of Degraded Documents for Long-Term Archival Using Waferfiche™ Technology

Basak Oztan[†], Gaurav Sharma[†], Ajay Pasupuleti^{*}, and P. R. Mukund^{*}

[†]ECE Dept., University of Rochester, Rochester, NY, 14627, ^{*}NanoArk Corporation, 125 Tech Park Dr., Rochester, NY, 14623
{basak.oztan,gaurav.sharma}@rochester.edu, {apasupuleti,prmukund}@nanoarkcorp.com

Abstract

Adaptive binarization techniques are proposed for the restoration of degraded documents for Waferfiche™ archival. Waferfiche™ is a compact archival solution for long-term preservation of documents in a human-accessible image based format. Bi-level images are preferable for the lithographic fabrication utilized in Waferfiche™ production. Binarization of degraded documents poses challenges due to the tonal variations in the foreground text and background paper. Using dispersion and edge based measures, our methods are specifically optimized for preserving information while eliminating unwanted noise. In addition, we present several pre/post-processing techniques that improve image quality. The effectiveness of our methodology is experimentally demonstrated by images captured from Waferfiches. Adaptive binarization using dispersion and edge based noise elimination thus provide an effective restoration method for degraded documents for Waferfiche™ archival.

1 Introduction

Archival is commonly necessary for documents that have historical significance or long-enduring value such as legal records, estate plans, transcripts/diplomas, medical documents, and historic manuscripts. Long-term preservation is, however, a challenging problem. Machine readable digital media and formats [1] face a constant cycle of technological upheaval that severely limits their longevity. On the contrary, common human-accessible media such as paper require an excessive amount of storage space. Though the storage space is significantly reduced by various forms of film based optical image storage systems [2], both paper and film based media suffer from severe physical degradation over time. In particular, microfilm archival [3], which has commonly been used for the long-term storage and preservation of documents, may encounter severe shortening in its expected lifespan upon an increase in the temperature and relative humidity of the storage facility [4,5]. Consequently, compact and robust human-accessible archival methods are desirable.

Waferfiche™ is an encouraging novel innovation developed for robust long-term archival of documents. The information is archived on a metal coated silicon wafer by imprinting images using microfabrication technology that is extensively utilized in integrated circuit fabrication. This silicon based medium is known to have a long lifetime. For instance, during the *Apollo 11* lunar mission, a silicon disc etched with goodwill messages was left on the surface of the moon [6]. Silicon is highly resistant to the variations in temperatures, humidity, and moisture thereby it is a versatile media for long-term preservation of information in physically challenging conditions. In fact, for the Waferfiche™ technology, a lifetime of over 500 years has been reported [7]. Microfabrication of archival images enables com-

compactness in Waferfiche™ archival, where, for example, an archiving capacity over 2500 letter-size documents can be reached on a standard six-inch wafer using 2μm (or finer) fabrication technology. As with other methods, the information is preserved in a human-accessible format since its recovery requires only the use of suitable optical magnification. For purpose of illustration, Fig. 1 shows a sample Waferfiche™ containing historic “Sarvamoola Grantha” manuscripts.

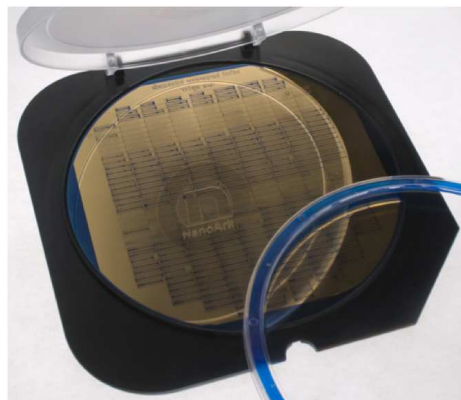


Figure 1. Sample Waferfiche™ archiving medium.

Binary images are preferable in the microfabrication of Waferfiche™. Documents for Waferfiche™ can come from multiple sources including microfilms, original hardcopy records, and electronically generated documents. For a majority of documents, where the originals are in good condition, the preprocessing for Waferfiche™ archival is straightforward. However, degraded documents pose several challenges that we address in this work. Specifically, images that are severely deteriorated due to aging and less than optimal storage are considered in our work. These images typically exhibit significant foreground and background variations in tones in addition to noise. We develop adaptive binarization techniques specifically optimized for maximally preserving text information in the transfer to the more robust Waferfiche™ medium. We present experimental results demonstrating the efficacy of our methods comparing images of degraded documents with their binarized counterparts and with images retrieved from Waferfiches obtained using these methods.

2 Overview of Waferfiche™ Archiving Technology

An overview of Waferfiche™ archival process is illustrated in Fig. 2. Documents on different media are first captured by devices with suitable resolution as continuous tone (contone) im-

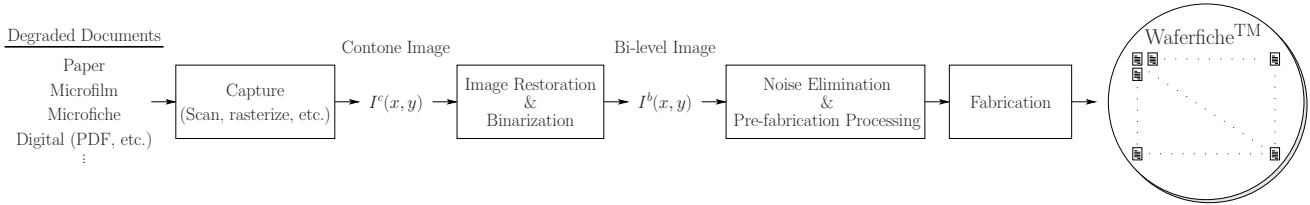


Figure 2. An overview of Waferfiche™ document archival process.

ages. In order to prepare these images for Waferfiche™ archival, bi-level representations for the captured contone images are obtained by binarization. As a result of the adaptive binarization method developed for maximally preserving information (described in Sec. 3.2), some amount of unwanted background noise is also generated in the binary representations of degraded documents. The unwanted noise is eliminated using the methods we describe in Secs. 3.3.1 and 3.3.2. In addition, using the techniques described in Sec. 3.5, the resulting images are prepared for Waferfiche™ fabrication. Finally, using microfabrication steps that include oxide deposition, metal deposition, photolithography and metal etching, bi-level images are archived on Waferfiche™.

3 Processing of Degraded Documents for Waferfiche™ Technology

3.1 Types of Degradations

The degraded documents that we encounter typically exhibit significant foreground and background variations in gray level in addition to extrinsic noise such as dirt. We observe degradations such as fading of ink/toner, non-uniform/inadequate ribbon ink for typewritten documents, ghost image appearance due storage of documents on top of each other, and other physical degradations on paper and film. In Fig. 3, we show portions of two documents, where foreground and background tonal values vary. These variations can also be observed on the normalized histograms shown in Fig. 4. As we describe in the next section, these variations pose challenges for the binarization of the images captured from degraded documents for Waferfiche™.

3.2 Document Binarization

Binarization separates the image values into two classes: foreground and background. In typical document images, foreground features include text, line drawings, pictures, etc., and the background is usually the paper. Binarization for a document image should, therefore, maximally preserve the text while eliminating the noise on the paper. Misclassifications may degrade the legibility of the document and, therefore, choice of the binarization technique is a crucial step.

The binary image $I^b(x, y)$ is obtained by comparing the contone image values $I^c(x, y)$ against a threshold function $T(x, y)$, where x and y represent the spatial coordinates along the horizontal and vertical directions, respectively. Specifically

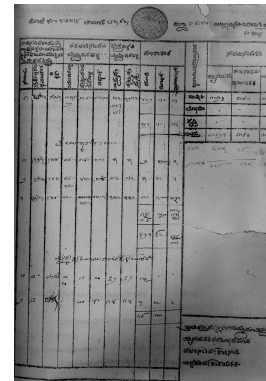
$$I^b(x, y) = \begin{cases} 1 & \text{if } I^c(x, y) > T(x, y), \\ 0 & \text{otherwise,} \end{cases} \quad (1)$$

defines the binary image, where the values 0 and 1 correspond to the image levels for the foreground and background, respectively.

Several binarization techniques have been proposed in the literature [8]. The characteristics of the document, specific application requirements, and computational complexity are some of

COURSE NUMBER	COURSE TITLE	CREDITS	COURSE NUMBER	COURSE TITLE	CREDITS
MA 101	FALL STR 1961-62	3	MA 103	FALL STR 1962-63	3
MA 121	CALCULUS	4	MA 201	CALCULUS	4
MA 102	MACH TOOL LABORATORY	1	MA 202	CALCULUS	4
MA 103	COMMUNICATION SKILLS	1	MA 203	PHYSICS	4
MA 104	GENERAL CHEMISTRY	4	MA 204	PHYSICS	4
MA 105	WESTERN CIVILIZATION	3	MA 205	HEAT POWER	4
MA 106	ENGINEERING DRAWING	3			
MA 107	ACAD PROB	1			
MA 122	WINTER STR 1961-62	3			
MA 141	MACH TOOL	1			
MA 142	ENG DRAW	1			
MA 102	WESTERN CIVILIZATION	3			
MA 101	PSYCHOLOGY	3			
MA 101	CALCULUS (S)	3			
MA 100	GENERAL CHEM	4			
	SPRING STR 1961-62	3			
MA 102	PRECISION MEASUREMENT	1			
MA 103	COMMUNICATION SKILLS	1			
MA 104	GENERAL CHEM	4			
MA 105	CALCULUS	4			
MA 106	PSYCHOLOGY	3			
MA 107	GENERAL CHEM	4			
MA 108	GRAPHICAL ANALYSIS	1			
MA 109	MACH TOOL LAB	1			
	FALL STR 1963-64	2			
	COOP EMPLOYMENT	2			

(a)



(b)

Figure 3. Examples of degradations encountered. Document (a), obtained from a microfilm scan, shows fading in foreground tonal values; and document (b), scanned from hardcopy, shows variations in background.

the common factors that impact the choice of a binarization technique. Since a large number of images that need to be processed for archival, we seek a simple but efficient algorithm. In particular, we use an adaptation of Otsu's well-known binarization method [9] to determine the threshold function $T(x, y)$, wherein the method is either utilized globally or adapted locally in order to better handle spatial variations in foreground-background contrast.

Otsu's method [9] chooses a single threshold value ($T(x, y) = T_{opt}$) for an image that minimizes the *intra-class variance* between the foreground and background classes. For image values between 0 and 255, this computation is given as

$$T_{opt} = \arg \max_T \frac{P(T)(1 - P(T))(\mu_f - \mu_b)^2}{P(T)\sigma_f^2 + (1 - P(T))\sigma_b^2}, \quad (2)$$

where $P(T) = \sum_{t=0}^T p(t)$ is the cumulative image histogram, μ_f and μ_b are the mean values over the foreground and background partitions, respectively, when thresholding at the gray level T , and σ_f^2 and σ_b^2 are the variances over the foreground and background partitions, respectively, when thresholding at the gray level T .

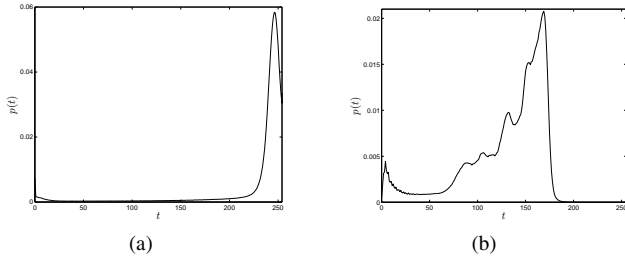


Figure 4. Normalized histograms of images captured from degraded documents. (a) and (b) show the histograms of the images in Fig. 3(a) and (b), respectively.

For purpose of illustration, Fig. 5(a) shows the binary representation obtained by binarizing the image using the Otsu thresholding in Eq. (1). The optimal threshold value T is computed as 151 and 109 using the normalized histograms shown in Fig. 4(a) and (b), respectively. One can readily see the high contrast information in the contone images is nicely preserved, whereas significant information in low contrast regions is lost. Hence, while global binarization may be effective for documents that do not exhibit variations in the foreground and background tonal values, for most degraded documents, loss of information should be expected.

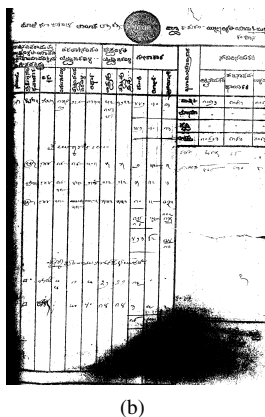
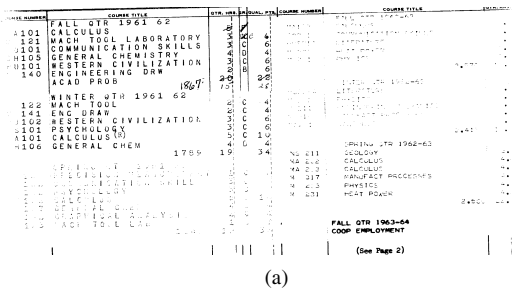


Figure 5. (a) and (b) show global binarization results for the images in Fig. 3(a) and (b), respectively.

In the presence of spatial variations in contrast, such as those seen in Fig. 3, low contrast information can be preserved by local binarization. An overview of local binarization is shown in Fig. 6. The contone image is first divided into M_x and M_y constant size rectangular blocks along the horizontal and vertical directions, respectively. Next, each block is binarized using a blockwise con-

stant threshold computed by Otsu's method¹, where

$$I^b_{(i,j)}(x,y) = \begin{cases} 1 & \text{if } I^c_{(i,j)}(x,y) > T_{(i,j)}, \\ 0 & \text{otherwise,} \end{cases} \quad (3)$$

defines the binary representation for the $(i,j)^{th}$ block, $i \in \{1, 2, \dots, M_x\}$ and $j \in \{1, 2, \dots, M_y\}$, where $T_{(i,j)}$ is the optimal threshold value for the $(i,j)^{th}$ block. $T_{(i,j)}$ is computed by using Eq. (2) with the normalized histogram $p_{(i,j)}(t)$ of the $(i,j)^{th}$ block. The final binary image $I^b(x,y)$ is obtained by tiling the binarized blocks accordingly. Equivalently, it can also be obtained via Eq. (1) using a threshold for the contone image $I^c(x,y)$ defined by $T(x,y) = T_{(i(x),j(y))}$, where $i(x) = \lceil \frac{x}{M_x} \rceil$ and $j(y) = \lceil \frac{y}{M_y} \rceil$ represent the threshold for the $(i,j)^{th}$ block, where $\lceil \cdot \rceil$ is the ceiling function that maps its argument to the next largest integer.

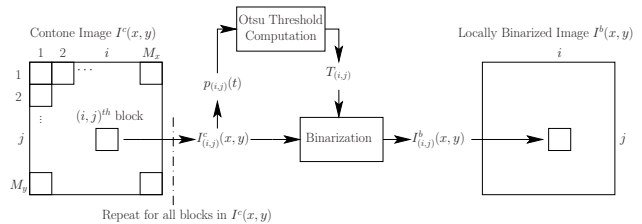


Figure 6. Local binarization process.

Figures 7(a) and (b) show the locally binarized images obtained with $M_x = M_y = 64$. It is clear that a significant amount of low contrast information that is lost due global binarization (compare against Figs. 5(a) and (b)) is preserved by local binarization. However, objectionable background noise is produced due to the binarization of local regions that contain hardly no information. In order to eliminate these noise, we develop two techniques that we describe next.

3.3 Noise Elimination

In order to eliminate the noise in the locally binarized image, we need to distinguish between the information arising from the document content and noise arising due to the contrast adaptive local processing. Document content is more structured than the unwanted noise. Therefore, we develop methods to evaluate the structuredness of the information to eliminate the unwanted noise.

3.3.1 Dispersion Based Noise Elimination

Our first method uses the spatial content within each block to infer whether the binary information in a block is, or is not, structured. The information in a block is considered as the realization of a spatial point process, where the observed pattern is classified as either *random*, *regular*, or *clustered* [11]. Clustered patterns are considered as structured and preserved, and the other types of patterns are considered as unstructured and eliminated. For this purpose, a measure of dispersion [12] is computed for each block $I^b_{(i,j)}$, $i \in \{1, 2, \dots, M_x\}$ and $j \in \{1, 2, \dots, M_y\}$ in $I^b(x,y)$. The dispersion based noise eliminated binary image is defined by

$$I^b_{disp}(x,y) = \begin{cases} I^b(x,y) & \text{if } D_{(i,j)} > D_{thr}, \\ 1 & \text{otherwise,} \end{cases} \quad (4)$$

¹For computational reasons, instead of computing a threshold value for each pixel [10], blockwise constant thresholding is preferred.

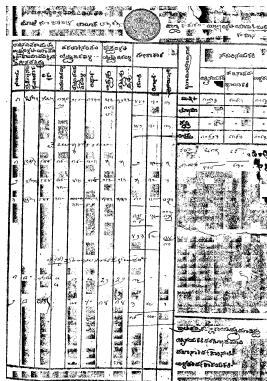
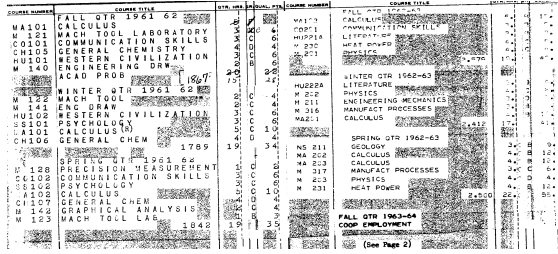


Figure 7. (a) and (b) show local binarization results for the images in Fig. 3(a) and (b), respectively, obtained with $M_x = M_y = 64$.

where $D_{(i,j)}$ is the dispersion measure for the $(i,j)^{th}$ block where the pixel (x,y) is located, and D_{thr} is the dispersion threshold. It can be inferred that as the dispersion threshold D_{thr} increased, unstructured noise is progressively removed, however, useful information in a block can also be eliminated. Therefore, while the threshold D_{thr} should be high enough to remove the unstructured noise, it should also be low enough to preserve information.

We use quadrat analysis method to compute the dispersion measure [11]. An overview of the computation of the dispersion measure $D_{(i,j)}$ for the block $I^b_{(i,j)}$ is shown in Fig. 8. First, the image is divided into Q_x and Q_y small rectangular blocks, referred to as *quadrats*. Next, the count of events in the each quadrat is stored in $C(p,q)$, $p \in \{1, 2, \dots, Q_x\}$ and $q \in \{1, 2, \dots, Q_y\}$. The dispersion measure is then computed as²

$$D_{(i,j)} = \frac{\sigma^2_{(i,j)}}{\mu_{(i,j)}} - 1, \quad (5)$$

where $\mu_{(i,j)}$ and $\sigma^2_{(i,j)}$ are the sample mean and variance of the counts of events $C(p,q)$ in the binary block $I^b_{(i,j)}$, respectively. The dispersion measure $D_{(i,j)}$ can take values between -1 and $q_x \times q_y - 1$, where q_x and q_y are the size of the quadrat along the horizontal and vertical directions, respectively. Smaller dispersion measure values correspond to non-structured information, whereas larger values represent structured features.

Figure 9 shows the binary image obtained by locally binarizing the contone image of Fig. 3(a) with $M_x = M_y = 64$ after elimination of noise using the dispersion based approach using 3×3 pixel quadrats and $D_{thr} = 2.5$. It is clear that unwanted noise observed in Fig. 7(a) is considerably reduced, while the foreground text is preserved.

²This dispersion measure is also known as “index of clumping” [12].

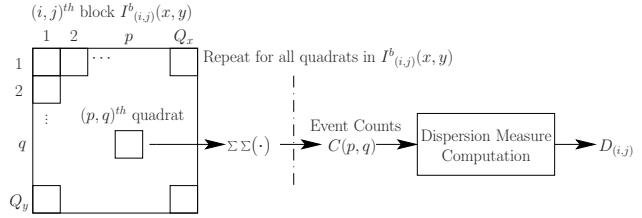


Figure 8. Dispersion measure computation.

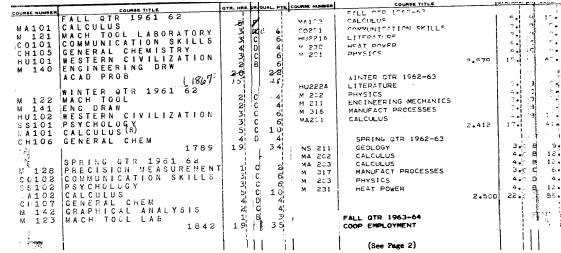


Figure 9. Image of Fig. 7(a) after dispersion based noise elimination.

3.3.2 Edge Based Noise Elimination

Our second method employs an edge based noise removal. Documents often contain edges due text or line drawings. Therefore, structuredness of the document content can be determined using the edges in the image. For this purpose, we use the number of edges within each block to assess the presence of information. Information in a block with low number of edges is considered unwanted noise and removed, and, similarly, the information in a block with large number of edges is referred to as structured and preserved. An overview of edge based noise elimination is shown in Fig. 10. The edge based noise eliminated binary image is defined by

$$I^b_{edge}(x,y) = \begin{cases} I^b(x,y) & \text{if } \overline{I^e_{(i,j)}(x,y)} > \epsilon, \\ 1 & \text{otherwise,} \end{cases} \quad (6)$$

where $\overline{I^e_{(i,j)}(x,y)}$ is the expected value of a binary “edge map” $I^e(x,y)$ over the $(i,j)^{th}$ block, where the pixel (x,y) is located, and ϵ is a threshold value.

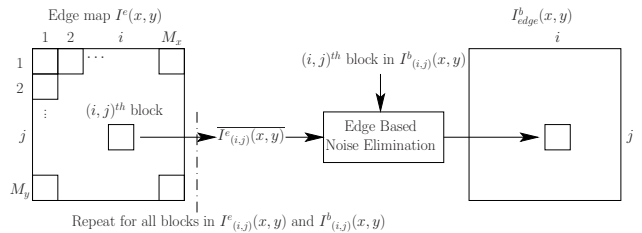


Figure 10. Edge based noise elimination.

The binary edge map $I^e(x,y)$ is obtained by edge detection [13]. Specifically,

$$I^e(x,y) = \begin{cases} 1 & \text{if } G(x,y) > E_{thr}, \\ 0 & \text{otherwise,} \end{cases} \quad (7)$$

defines the edge map, where the value 1 and 0 correspond to the presence and absence of edge, respectively, and E_{thr} is a threshold to assess significance of edges and $G(x,y)$ is the magnitude of image gradient computed by $|\nabla G(x,y)| = \sqrt{G_x^2(x,y) + G_y^2(x,y)}$,

where $G_x(x, y)$ and $G_y(x, y)$ are the first-order image derivatives along the horizontal and vertical directions, respectively. Approximations to these functions can be obtained by using linear shift-invariant filters as $G_x(x, y) = I^c(x, y) * g_x(x, y)$ and $G_y(x, y) = I^c(x, y) * g_y(x, y)$, where g_x and g_y are the filters to compute image gradients, and $*$ represents 2D convolution operation. Several filters are proposed for the estimation of the directional image gradients G_x and G_y [13]. In this paper, we use the well-known *Sobel operators* [13] to compute the directional image gradients.

Figure 11(a) shows the binary edge map $I^e(x, y)$ for the image of Fig. 3(b) obtained with $E_{thr} = 80$ via Eq. (7) and Fig. 11(b) shows the edge based noise eliminated image by locally binarizing the contone image of Fig. 3(b) with $M_x = M_y = 64$, and eliminating unwanted noise within each block using $\epsilon = 0.008$. It is clear that unwanted noise observed in Fig. 7(b) is considerably reduced, while the foreground text is preserved.

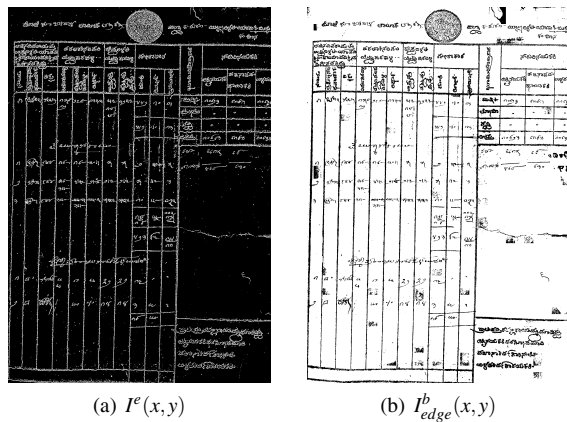


Figure 11. Edge based noise elimination for the image of Fig. 7(b).

Both adaptive binarization techniques have advantages. While binarization using dispersion measure is more efficient in handling tonal variations in the text, binarization with edge detection is more useful in handling line drawings and degradations in the background. Therefore, in practice, we utilize a suitable combination of the two approaches.

3.4 Binarization of Color Documents

For the bi-level representation of color documents, one may trivially capture the document as a gray level image and perform the binarization subsequently. The information in each color channel, however, may not be consistent and during the transformation from color to gray, low contrast information in the individual color channels may not translate. This may yield loss of information and should be avoided. The information in the individual color channels can be maximally preserved by binarizing each color channel separately and superposing the resulting bi-level representations to obtain the final binary image. For a typical RGB captured image, the final binary representation can be obtained as $I^b(x, y) = I^b_R(x, y) \wedge I^b_G(x, y) \wedge I^b_B(x, y)$, where $I^b_i(x, y)$ is the bi-level representation for the color channel i , $i \in \{R, G, B\}$, and \wedge is the logical AND operation.

3.5 Pre/Post-Processing

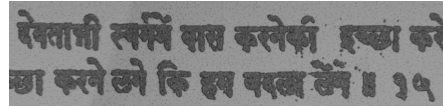
The bi-level image data is transferred to Waferfiche™ using lithographic fabrication. Due to imperfections in the microfabrication, the ideal non-overlapping square shaped pixels in the image enlarge and overlap non-uniformly on the Waferfiche™. This yield

a non-linear “process gain”, which typically yields thickened features³. Fig. 12(a) shows a portion of the bi-level representation for the historic “Vaishnava” script and Fig. 12(b) shows the corresponding portion of the image captured from the Waferfiche™. It can be seen that characters are generally thickened and filled. This behavior can be corrected by characterizing the system behavior and calibrating the parameters accordingly. A similar process gain is observed in the printing systems that has been studied extensively [14, 15]. There exists simple methods [16, 17] that can be adapted for the calibration of the parameters against the process gain. In addition, spectrophotometric response of the Waferfiche™ media can also be utilized to improve foreground-background contrast [18].

In this paper, however, we employ morphological image transforms, which have been extensively used in document image analysis [19], to compensate for the process gain. In particular, we use the *dilation* and *erosure* operators [13] in order to thin the features in the bi-level representations before Waferfiche™ fabrication and remove noise amplified by the process gain after the archived images are retrieved from Waferfiches. Figure 12(c) shows the binary image obtained by dilating the image of Fig. 12(a). It is clear that the features are thinned, however, these features are restored by the process gain during the fabrication.

देवताभी स्वर्गमें वास करनेकी इच्छा करे
छा करने लगे कि हम बदल लें ॥ १५

(a) Binary Vaishnava image



(b) Vaishnava image captured on Waferfiche™

देवताभी स्वर्गमें वास करनेकी इच्छा करे
छा करने लगे कि हम बदल लें ॥ १५

(c) Dilated Vaishnava binary image

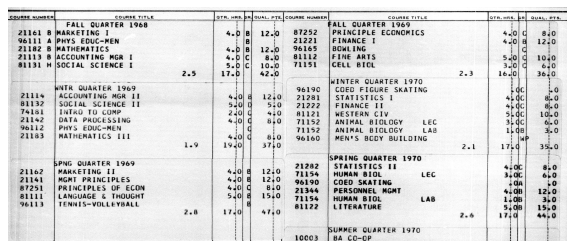
Figure 12. Illustration of pre-processing to compensate for the process gain. (a) shows portion of binary Vaishnava image, (b) shows image captured from the Waferfiche™, and (c) shows the binary image (a) after morphological dilation.

4 Experimental Results

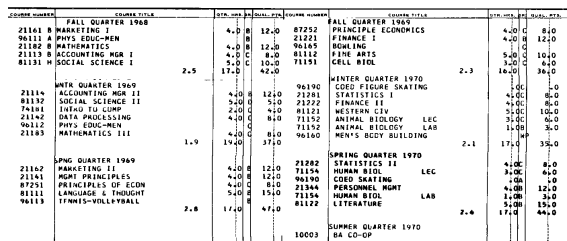
Our experimental setup utilized a microfilm scanner at 300×300 dpi resolution. First, we captured a large set of document images from microfilms. In general, captured images exhibit tonal variations in the foreground and background similar to the image of Fig. 3(a). We tuned the parameters of the adaptive binarization algorithms for the optimal preservation of the information in these types of documents. Fig. 13(a) shows a sample portion of the contone *Transcript* image scanned from a microfilm and Fig. 13(b) demonstrates the optimized binary representation for this image obtained using our processing technique. It can be

³Depending on the microfabrication method, it can also yield thinned features.

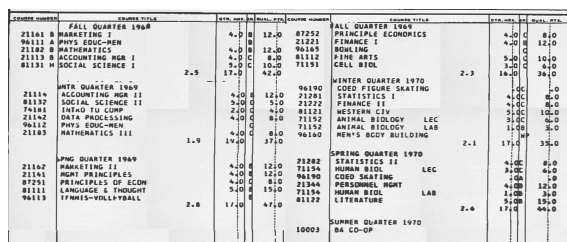
clearly seen that the information in Fig. 13(a) is maximally preserved and the binary image do not contain any unwanted noise. Next, a set of binary images were archived on Waferfiche™ using 2 μm lithographic fabrication technology and archived images were captured through a microscope with 10× optical magnification for demonstration. Figure 13(c) shows the archived Transcript image captured from the Waferfiche™ that indicates that the information is well-preserved in the archiving process.



(a) Contone Transcript image



(b) Binary Transcript image



(c) Transcript image captured on Waferfiche™

Figure 13. Experimental results. (a) shows the original contone image, (b) shows the binary representation of (a), and (c) shows the image archived on the Waferfiche™ medium.

5 Conclusion

In this paper, we present techniques for processing degraded document images for long-term archival using Waferfiche™ technology. In particular, we present adaptive binarization techniques aimed at maximally preserving information while eliminating unwanted background noise. In addition, using pre and post-processing techniques we demonstrate improvements on the quality of the restored information. Experimental results demonstrated the efficacy of our methodology.

Acknowledgments

This work is supported by a grant from NanoArk Corporation and a partly matching grant from New York State Office of Science, Technology & Academic Research (NYSTAR) through the Center for Electronic Imaging Systems (CEIS) of University of Rochester.

Authors would also like to thank Dr. Vanditha Mukund and Mr. Ravi Nareppa of NanoArk Corp. for discussions, suggestions, and their help in tuning the experimental parameters.

References

- [1] L. Rosenthaler, "The (short) history of digital archiving," in *IS&T Archiving 2006*, pp. 69–74.
- [2] W. Saffady, *Micrographics*, 1st ed. Littleton, CO: Libraries Unlimited, 1978.
- [3] N. Gwinn and L. Fox, Eds., *Preservation microfilming: a guide for librarians and archivists*, 2nd ed. Chicago, IL: American Library Association, 1996.
- [4] ISO 18911:2000, "Imaging materials – processed safety photographic films – storage practices," 2000.
- [5] ISO 18901:2002, "Imaging materials – processed silver-gelatin type black-and-white films – specifications for stability," 2002.
- [6] T. Rahman, *We Came in Peace for all Mankind—the Untold Story of the Apollo 11 Silicon Disc*, 1st ed. Overland Park, KS: Leathers Publishing, 2008.
- [7] D. Burge, "Report on the Image Stability Test for Silicon/Deposited Aluminum Microfiche," Image Permanence Institute, Rochester, NY, Tech. Rep., June 9, 2007.
- [8] M. Sezgin and B. Sankur, "Survey over image thresholding techniques and quantitative performance evaluation," *J. Electronic Imaging*, vol. 13, no. 1, pp. 146–165, Jan. 2004.
- [9] N. Otsu, "A threshold selection method from gray-level histograms," *IEEE Trans. Sys., Man, and Cyber.*, vol. 9, no. 1, pp. 225–236, Jan. 1979.
- [10] J. Sauvola and M. Pietikäinen, "Adaptive document image binarization," *Patt. Recogn.*, vol. 33, pp. 225–236, 2000.
- [11] N. A. Cressie, *Statistics for Spatial Data*. New York: Wiley, 1993.
- [12] G. Upton and B. Fingleton, *Spatial Data Analysis by Example, Vol. I, Point Pattern and Quantitative Data*. New York, NY: Wiley, 1985.
- [13] R. C. Gonzalez and R. E. Woods, *Digital Image Processing*, 2nd ed. Upper Saddle River, NJ: Prentice-Hall, 2002.
- [14] J. A. C. Yule, *Principles of color reproduction, applied to photomechanical reproduction, color photography, and the ink, paper, and other related Industries*. New York: Wiley, 1967.
- [15] G. Sharma, Ed., *Digital Color Imaging Handbook*. Boca Raton, FL: CRC Press, 2003.
- [16] S. Wang and K. T. Knox, "Novel centering method for overlapping correction in halftoning," in *IS&T's 47th Annual Conference, ICPS'94: The Physics and Chemistry of Imaging Systems*, vol. 2, 15–20 May 1994, pp. 482–486.
- [17] K. R. Crouse, "Measurement-based printer models with reduced number of parameters," in *Proc. SPIE: Color Imaging: Device Independent Color, Color Hardcopy, and Applications VII*, R. Eschbach and G. G. Marcu, Eds., vol. 4663, Jan. 2002, pp. 121–129.
- [18] J. Henrie, S. Kellis, S. Schultz, and A. Hawkins, "Electronic color charts for dielectric films on silicon," *Optics Express*, vol. 12, no. 7, pp. 1464–1469, 2004.
- [19] R. P. Loce and E. R. Dougherty, *Enhancement and Restoration of Digital Documents: Statistical Design of Nonlinear Algorithms*. Bellingham, WA: SPIE Press, 1997.

Author Biography

Basak Oztan is a PhD candidate in the Department of Electrical and Computer Engineering, University of Rochester, Rochester, New York. He was with Xerox Webster Research Center, Webster, New York, during the summers of 2005 and 2006 as a research intern. He is the recipient of a student paper award at IEEE ICASSP 2006 in the image and multi-dimensional signal processing category. His research interests include color imaging, color halftoning, and multimedia security. Mr. Oztan is a student member of IS&T, SPIE, IEEE, and the IEEE Signal Processing Society.